Linear-Regioselective Hydromethoxycarbonylation of Styrene Using Ru-Clusters/CeO_2 Catalyst

Jinghua An[a,b], Yehong Wang[a], Zhixin Zhang[a], Jian Zhang[a], Martin Gocyla[c], Rafal E. Dunin-Borkowski[c], and Feng Wang[a,*]

[a] State Key Laboratory of Catalysis, Dalian National Laboratory for Clean Energy, Dalian Institute of Chemical Physics, Chinese Academy of Sciences, 457 Zhongshan Road, Dalian 116023, China

[b] University of Chinese Academy of Sciences, Beijing 100049, China

c Ernst Ruska Centre for Microscopy and Spectroscopy with Electrons and Peter Grünberg Institute, Forschungszentrum Juelich GmbH, Juelich 52425, Germany

Abstract: Hydroalkoxycarbonylation of olefins has been considered to be one of the most attractive methods to synthesize esters. Controlling the regioselectivities of linear esters (**L**) and branched esters (**B**) is a challenging project for researchers working in this reaction. Although most of the attention has been paid to control the regioselectivity through ligand design in homogeneous catalytic systems, study in the area is still limited. Herein, Ru-clusters/CeO_2 is employed as a heterogeneous catalyst for the hydromethoxycarbonylation of styrene without any additives. After optimization of the reaction conditions, the conversion of styrene is > 99% with 83% and 12% regioselectivity of linear and branched ester, respectively. By using different supports (CeO_2 (nanoparticle), CeO_2-rod and CeO_2-cube), three catalysts including Ru-clusters/CeO_2, Ru/CeO_2-rod, and Ru/CeO_2-cube are prepared and applied in the reaction. Structural characterizations demonstrate that the **L**/**B** ratio is related to the Ru size of supported Ru catalysts. Further Raman characterization and NH_3-TPD demonstrate that the metal-support interaction and the concentration of oxygen vacancy of the catalyst have a great influence on the Ru size. The mechanism and kinetic analysis for this reaction are also investigated in this work.

Key words: regioselectivity; Ru-clusters/CeO_2; ester; hydromethoxycarbonylation; olefins; heterogeneous.

Received XXXX-XX-XX. Accepted XXXX-XX-XX. Published XXXX-XX-XX.

*Corresponding author. Tel: +86-411-84379798; Fax: +86-411-84379798; E-mail: wangfeng@dicp.ac.cn

This work was supported by the Strategic Priority Research Program of the Chinese Academy of Sciences (XDB17020300), the National Natural Science Foundation of China (21721004, 21690084, and 21690080).

Esters exist in various natural products such as green olives, pears and have numbers of applications on the production of perfumes and flavorings et. al [1]. Consequently, various methods have been reported to synthesize esters such as the esterification of carboxylic acids with alcohols [2], the condensation of acid chlorides and alcohols [3] as well as the alcoholysis of nitriles [4]. Compared with those methods, the

functionalization of olefins in the presence of carbon monoxide (CO) and alcohols, which is named as hydroalkoxycarbonylation of olefins, has been considered to be one of the most attractive methods synthesizing esters owing to the 100% of the atom economy, and the using of readily available starting materials [5-15].

Controlling regioselectivity is a challenging project for chemists working in hydroalkoxycarbonylation of olefins [9, 15-16]. Numerous researchers have attempted to control the regioselectivity through ligand design or modification in homogeneous catalytic systems. For example, monodentate N-phenylpyrrole phosphine ligand was designed by M.Beller group and applied in hydroalkoxycarbonylation of olefins with high regioselectivities of branched esters owing to the steric hindrance of the ligand (up to 91%), which had been verified through the density functional theory (DFT) calculation (Scheme 1a) [1]. Although it is well known that monodentate phosphine ligands are favor to the production of branched esters, there are still some exceptions. Recently, a monodentate cage phosphaadamantane ligand in combination with Lewis acid such as $SnCl_2$ was reported to enhance the regioselectivities of the linear esters in the range of 70-96% when $PdCl_2$ was used as the catalyst (Scheme 1b) [17]. Additionally, considering the fact that more attention has been turned to heterogeneous catalytic system owing to the difficulties in the separation as well as reusability of homogeneous catalysts [18], the investigation of factors affecting the regioselectivity attracts more and more attention in heterogeneous catalytic system. Recently, there is one heterogeneous catalytic system reported in the literature and high regioselectivities of branched esters (up to 91%) were obtained with Pd-TPPTS-OTPPTS complex supported on acidic resin as the heterogeneous catalyst (Scheme 1c) [19-20]. They found that the reaction regioselectivity was remarkably impacted by the pore size of the support owing to the steric confinement effect [20]. Therefore, the development of a greener heterogeneous catalytic system with high activity and excellent regioselectivity, especially of linear esters, as well as the in-depth investigating of the factors affecting regioselectivity is urgent for the reaction.

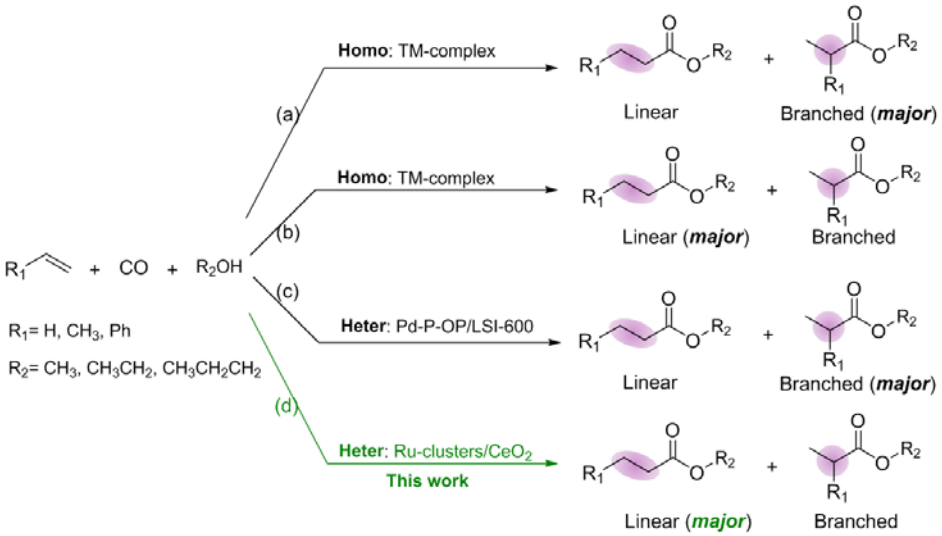

Scheme 1. Synthesis of esters via hydroalkoxycarbonylation of olefins. Homo: homogeneous catalyst; Heter: heterogeneous catalyst.

In our previous works, Ru-clusters/CeO_2 has been used in various carbonylation reactions [21-23]. For example, we reported the synthesis of methyl propionate from hydromethoxycarbonylation of ethylene over Ru-clusters/CeO_2 catalyst [21]. Although excellent catalytic performance was obtained, there is no regioselectivity for methyl propionate. Herein, Ru-clusters/CeO_2 was used as the catalyst for hydromethoxycarbonylation of terminal olefin, that is, styrene, to investigate the factors influencing the regioselectivity. The conversion of styrene was > 99% and the regioselectivity of linear and branched ester was 83% and 12%, respectively (Scheme 1d). By using different supports (CeO_2 (nanoparticle), CeO_2-rod and CeO_2-cube), three catalysts including Ru-clusters/CeO_2, Ru/CeO_2-rod, and Ru/CeO_2-cube were prepared and applied in this reaction. Structural characterizations demonstrate that the **L**/**B** ratio is related to the Ru size of supported Ru catalysts. Raman characterization and NH_3-TPD results showed that the Ru size had a great relationship with the metal support interaction and the concentration of oxygen vacancy of the catalyst. The highest regioselectivity of linear ester could be obtained using Ru-clusters/CeO_2 as catalyst owing to the smallest size of Ru clusters on the CeO_2 surface.

Table 1. Hydromethoxycarbonylation of styrene.[a]

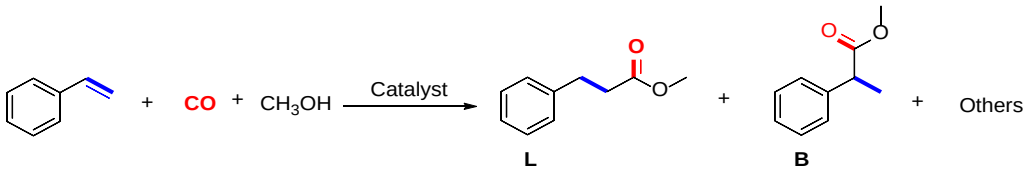

Entry	Catalyst	Conversion of styrene (%)	Product distribution (%)		
			L	B	Others
1	Ru-clusters/CeO_2	43	82	13	5
2	no catalyst	< 2	trace	trace	trace
3	CeO_2	< 2	trace	trace	trace
4	$RuCl_3 \cdot nH_2O$	> 99	36	6	58
5[b]	Pd/CeO_2	15	trace	trace	trace
6	Rh/CeO_2	< 2	trace	trace	trace
7	Ru/SiO_2	7	61	21	8

Reaction conditions: catalyst (0.1 g), styrene (0.5 mmol), methanol (4 ml), CO (0.9 MPa), 165 °C, 6 h. Conversion is determined by GC using mesitylene as an internal standard. CeO_2: CeO_2 nanoparticle. Other products are ethylbenzene and polystyrene. **L**: linear ester. **B**: branched ester. [b] The product is ethylbenzene.

Initially, hydromethoxycarbonylation of styrene was conducted under 0.5 MPa of CO in methanol at 165 °C for 6 h. When Ru-clusters/CeO_2 was used as the catalyst, the conversion of styrene was 43% with 82% and 13% regioselectivity of linear ester and branched ester, respectively (Table 1, entry 1). The reaction did not take place in the absence of catalyst or only in the presence of CeO_2 support (Table 1, entries 2–3). In comparison, $RuCl_3 \cdot nH_2O$, the precursor of the Ru for Ru-clusters/CeO_2, gave very low regioselectivity of total ester (**L**/**B** = 36:6), albeit > 99% conversion of styrene (Table 1, entry 4). Other metals including Pd and Rh exhibited no activities at all (Table 1, entries 5–6). Both a low conversion of styrene (7%) and poor regioselectivity of 61:21 (**L**/**B)** were obtained when Ru/SiO_2 was used as the catalyst (Table 1, entries 7).

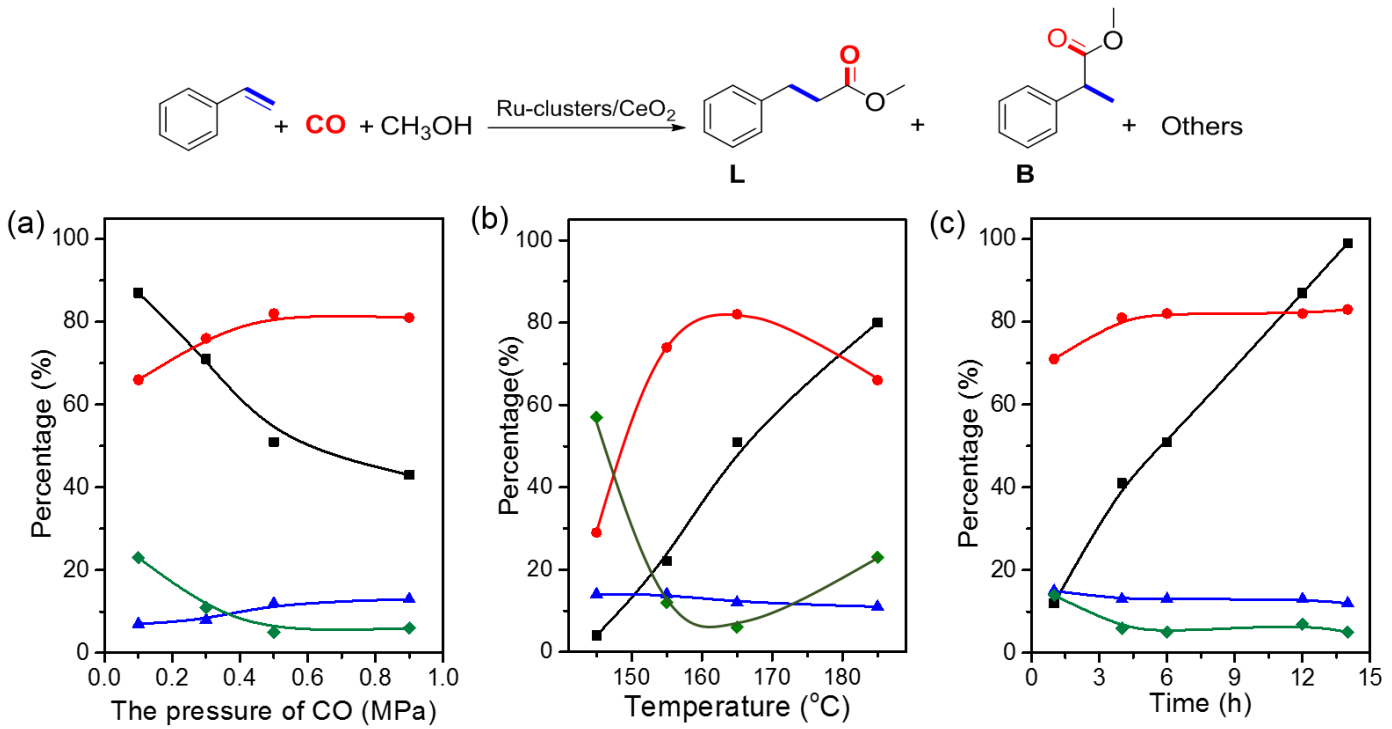

Fig. 1. (a) Effect of CO pressure on hydromethoxycarbonylation of styrene catalyzed by Ru-clusters/CeO_2. Reaction conditions: Ru-clusters/CeO_2 (0.1 g), methanol (4 ml), 165 °C, 6 h. Other products are ethylbenzene and polystyrene. (b) Effect of reaction temperature on styrene hydromethoxycarbonylation catalyzed by Ru-clusters/CeO_2. Reaction conditions: Ru-clusters/CeO_2 (0.1 g), methanol (4 ml), CO (0.5 MPa), 6 h. (c) Time-on-stream profile at 165 °C. Reaction conditions: Ru-clusters/CeO_2 (0.1 g), methanol (4 ml), CO (0.5 MPa), 165 °C. (■) Conversion of styrene, (●) Regioselectivity of linear ester, (▲) Regioselectivity of branched ester, (♦) Others.

Further experiments optimizing of the reaction conditions to improve catalytic activity were conducted (Fig. 1). First, we investigated the influence of CO pressure on styrene hydromethoxycarbonylation catalyzed by Ru-clusters/CeO_2 (Fig. 1a). Obviously, when the CO pressure increased from 0.1 to 0.9 MPa, the conversion of styrene was decreased from 87% to 43%. The regioselectivity of linear ester remained at 82% (**L**/**B** = 82:12). Therefore we chose 0.5 MPa as the optimizing pressure of CO, in which condition both a moderate conversion of styrene (51%) and high regioselectivity of 82:12 (**L**/**B**) could be obtained. Further

optimization of the reaction temperature under 0.5 MPa of CO was conducted (Fig. 1b). The catalytic results at temperatures of 145–185 °C showed that the conversion of styrene increased rapidly from 4% at 145 °C to 51% at 165 °C and then to 80% at 185 °C. The regioselectivity of 29:14 (**L**/**B**) obtained at 145 °C increased to 82:12 (**L**/**B**) at 165 °C and then decreased to 66:11 (**L**/**B**) at 185 °C. Thus the temperature of 165 °C was considered to be the optimal temperature for the reaction. Further extending the reaction time to 14 h under 0.5 MPa of CO at 165 °C, the conversion of styrene increased to > 99%, giving 83% and 12% regioselectivity of linear and branched ester, respectively (Fig. 1c).

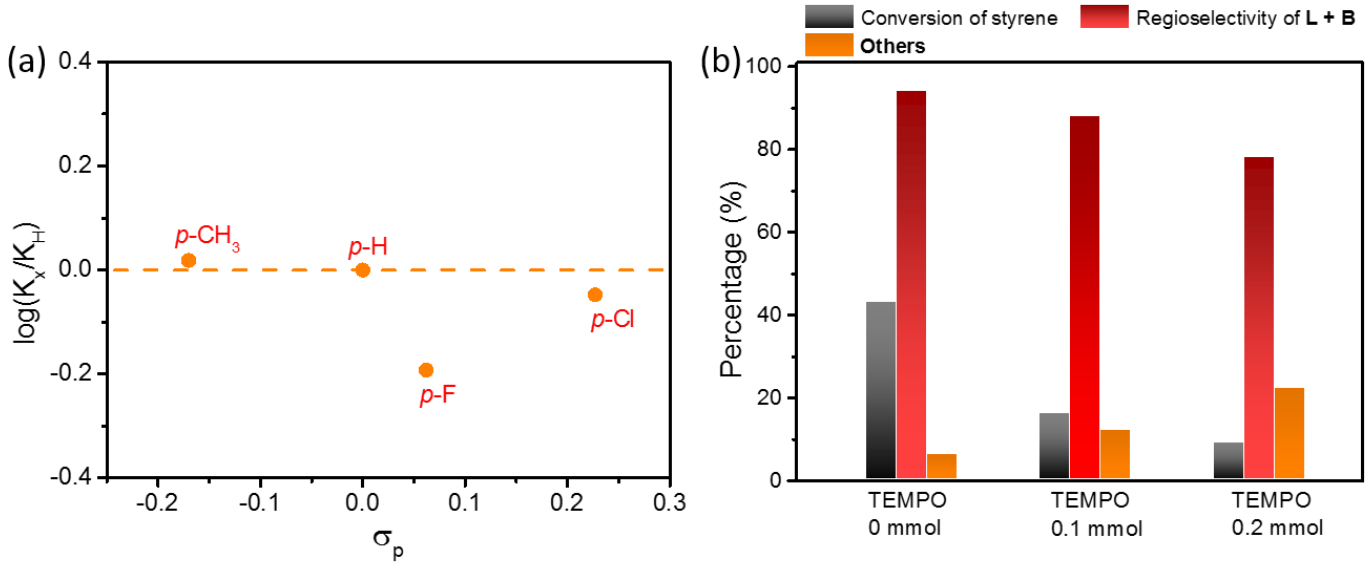

Fig. 2. Reaction mechanism investigations of hydromethoxycarbonylation of styrene over Ru-clusters/CeO_2. (a) Hammett plot, σ_p were obtained from literature [24]. Reaction conditions: Ru-clusters/CeO_2 (0.1 g), styrene or its derivative (0.5 mmol), methanol (4 ml), CO (0.5 MPa), 165 °C, 3 h. (b) The effect of the introduction of TEMPO. Reaction conditions: Ru-clusters/CeO_2 (0.1 g), styrene (0.5 mmol), methanol (4 mL), CO (0.9 MPa), 165 °C, 6 h. Other products are ethylbenzene and polystyrene.

Mechanism investigations for styrene hydromethoxycarbonylation over Ru-clusters/CeO_2 were then conducted (Fig. 2). Fig. 2a shows the plot of the logarithm of the rate constants $\log(k_X/k_H)$ plotted against Brown-Okamoto constant σ_p for each substituent on para-position in styrene (CH_3, H, F, or Cl). Obviously, there was no linear relationship between $\log(k_X/k_H)$ and σ_p, implying that the reaction is not sensitive to groups substituted on styrene [25]. Meanwhile, this result suggested the radical path of the reaction. Then further experiment using TEMPO (2,2,6,6-tetramethylpiperidine-N-oxide) as the radical inhibitor was conducted and the conversion of styrene decreased from 43% to 9% when 0.2 mmol of TEMPO was added into the reaction system, proving the radical path of hydromethoxycarbonylation of styrene over Ru-clusters/CeO_2 (Fig. 2b) [26-27].

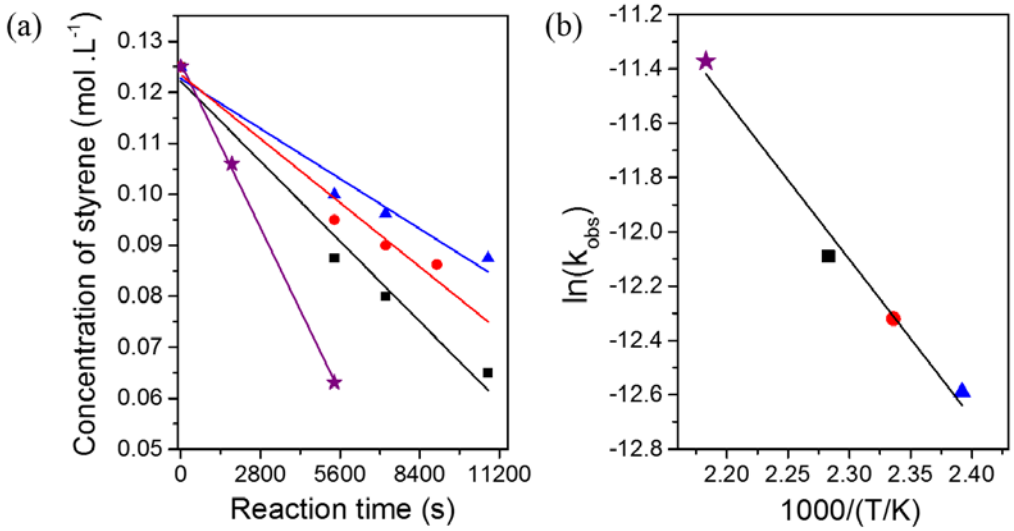

Fig. 3. (a) Kinetic analysis of styrene hydromethoxycarbonylation at (★) 175 °C, (■) 165 °C, (●)155 ℃, (▲) 145 °C using Ru-clusters/CeO_2 catalyst. (b) Arrhenius plot using the data in (a). Reaction conditions: Ru-clusters/CeO_2 (0.1 g), styrene (0.5 mmol), methanol (4 ml), CO (0.5 MPa).

The reaction kinetic of styrene hydromethoxycarbonylation was studied at temperatures of 145 °C–175 °C (Fig. 3a). The concentration of methanol, CO, and catalyst remained constant during the reaction, maintaining the dependence of the rate on styrene to be isolated. The k values at 175 °C, 165 °C, 155 °C, and 145 °C were 11.5×10^{-6}, 7.5×10^{-6}, 4.5×10^{-6}, and 5.6×10^{-6}, which were calculated from the slopes of the plots in Fig. 3a. Obviously, there was a linear Arrhenius plot of ln(k) versus 1000/T (Fig. 3b). And the activation energy (*Ea*) was calculated to be 48.50 KJ·mol^{-1}, indicating the smoothly proceeding of styrene hydromethoxycarbonylation over heterogeneous Ru-clusters/CeO_2 catalyst.

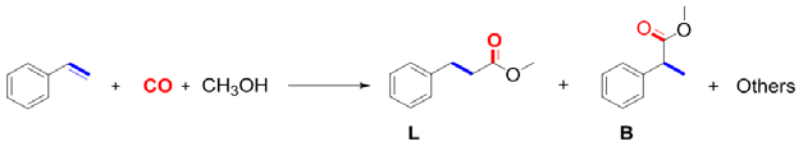

(a)

Catalyst	Conversion (%)	Product distribution (%)		
		L	B	Others
Ru/CeO_2-cube	23	66	21	13
Ru/CeO_2-rod	49	75	20	5
Ru-clusters/CeO_2	87	82	13	5

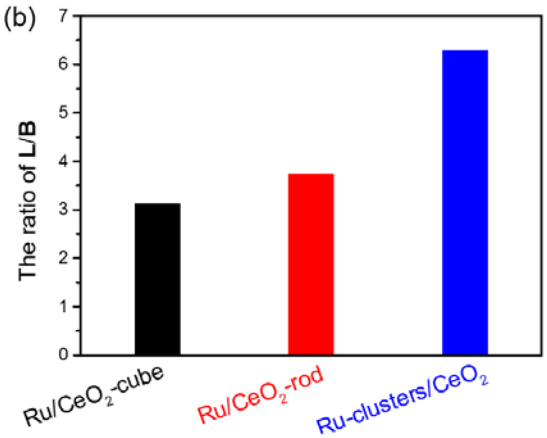

Fig. 4. (a) The catalytic performances of Ru-clusters/CeO_2, Ru/CeO_2-rod and Ru/CeO_2-cube on hydromethoxycarbonylation of styrene. Reaction conditions: Catalyst (0.1 g), methanol (4 ml), CO (0.5 MPa), 165 °C, 12 h. Other products are ethylbenzene and polystyrene. (b) The **L**/**B** ratios obtained in Fig. 4a.

In order to investigate the factors influencing the regioselectivity of styrene hydromethoxycarbonylation, three catalysts including Ru-clusters/CeO_2, Ru/CeO_2-rod and Ru/CeO_2-cube were prepared with the same method [28-31]. And then the three catalysts were applied in the hydromethoxycarbonylation of styrene under the same reaction conditions (Fig. 4a). When Ru/CeO_2-cube was used as the catalyst, the regioselectivity of 66:21 (**L**/**B**) was obtained. The reaction proceeded in higher regioselectivity of 75:20 (**L**/**B**) when Ru/CeO_2-rod was used as catalyst. A further higher regioselectivity of 82:13 (**L**/**B**) was achieved when Ru-clusters/CeO_2 was used as the catalyst. In order to show the difference of the regioselectivities over the three catalysts, **L**/**B** ratios were calculated and showed in Fig. 4b. The order of **L**/**B** ratios was in a subsequence of Ru-clusters/CeO_2 (6.92) > Ru/CeO_2-rod (3.75) > Ru/CeO_2-cube (3.14) (Fig. 4b), which means that the highest **L**/**B** ratio was obtained when Ru-clusters/CeO_2 was used as catalyst.

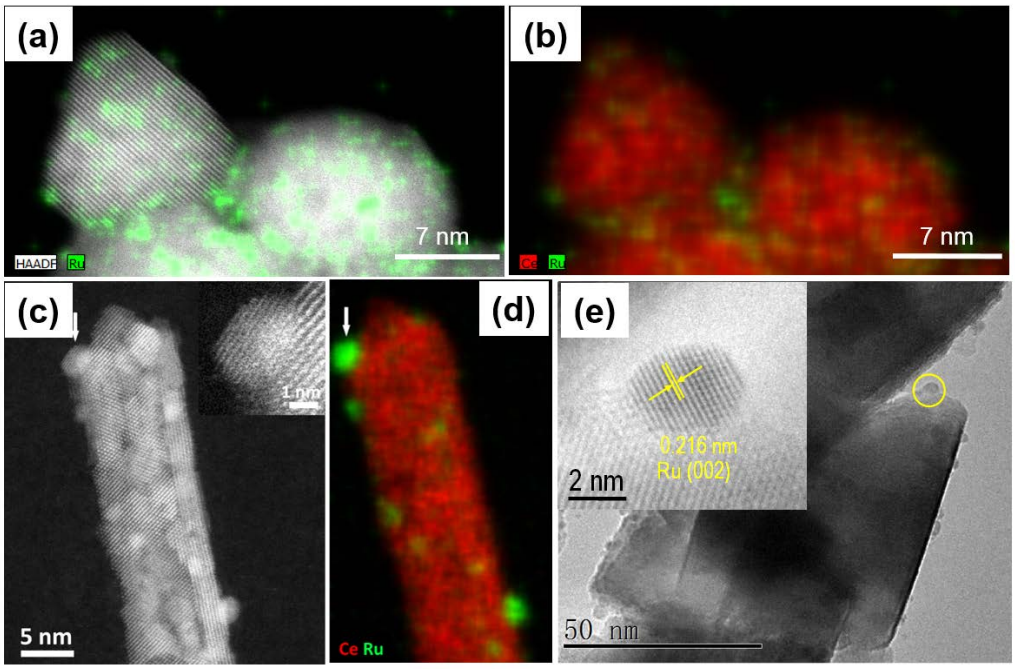

Fig. 5. (a) Combining HAADF-STEM image and EDX elemental mapping of Ru-clusters/CeO_2. (b) EDX elemental mapping of Ru-clusters/CeO_2. (c) HAADF-STEM images of Ru/CeO_2-rod. (d) EDX elemental mapping of Ru/CeO_2-rod. The inset shows an enlargement of the Ru nanoparticle indicated by white arrow. (e) The TEM and HR-TEM images of Ru/CeO_2-cube.

To elucidate the reasons for observed different **L**/**B** ratios obtained in hydromethoxycarbonylation of styrene over the three catalysts, we first characterized their structures using electron microscopy. Both high-angle annular dark-field imaging-transmission electron microscope (HADDF-STEM) and energy-dispersive X-ray spectroscopy (EDX) using the Ru L line confirmed that the highly-dispersed Ru clusters existed on the defected CeO_2 surface for Ru-clusters/CeO_2 (Fig. 5a and 5b). However, a small amount of Ru nanoparticles with most of Ru clusters could be observed on the surface of Ru/CeO_2-rod catalyst based on the characterizations from HADDF-STEM and EDX mappings using the Ru L line (Fig.

5c and 5d). The TEM and HR-TEM characterizations showed that a large number of Ru nanoparticles unevenly distributed on CeO_2-cube surface (Fig. 5e).

By combining the different Ru sizes and the **L**/**B** ratios obtained in styrene hydromethoxycarbonylation over the three catalysts, we found that the **L**/**B** ratio is related to the Ru size of supported Ru catalysts. The Ru-clusters/CeO_2, who has the smallest Ru size on CeO_2 surface, gave the highest **L**/**B** ratio in hydromethoxycarbonylation of styrene.

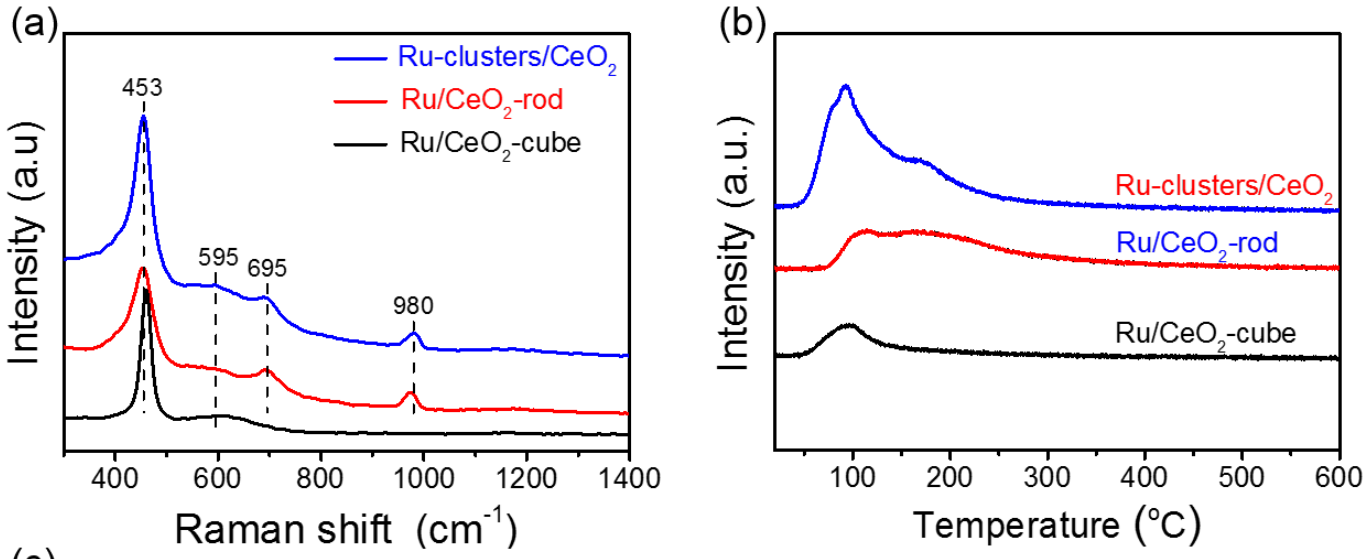

(c)

The order of concentration of oxygen vacancy	Ru-clusters/CeO_2 > Ru/CeO_2-rod > Ru/CeO_2-cube

Fig. 6. (a) The Raman characterization of the Ru-clusters/CeO_2, Ru/CeO_2-rod, and Ru/CeO_2-cube. (b) NH_3-TPD of Ru-clusters/CeO_2, Ru/CeO_2-rod and Ru/CeO_2-cube. (c) The order of concentration of oxygen vacancy.

Considering the fact that metal support interaction between metal and their oxide supports has profound effects on the dispersion and size of metal species in heterogeneous catalysts, the metal-support interaction for the three catalysts was then investigated *via* Raman characterization (Fig. 6a) [32-38]. The results were given in Fig. 6a and showed that the Ru-clusters/CeO_2, Ru/CeO_2-rod, and Ru/CeO_2-cube exhibited a strong peak at 453 cm^{-1} and a relative weaker peak at 595 cm^{-1}, corresponding to the vibration model of octahedral local symmetry around CeO_2 lattice and the defect-induced modes of CeO_2, respectively [39-43]. Besides the two peaks of CeO_2, two peaks at 695 cm^{-1} and 980 cm^{-1} were also observed for Ru-clusters/CeO_2 and Ru/CeO_2-rod, which could be assigned to Ru–O–Ce bond resulting from the stronger interaction between Ru species and the different supports (CeO_2 and CeO_2-rod) [44]. However, no peaks at 695 cm^{-1} and 980 cm^{-1} were observed in Ru/CeO_2-cube, indicating a weak interaction exists between Ru species and CeO_2-cube. Thus, the Raman characterization showed that there was a stronger metal support interaction in Ru-clusters/CeO_2 and Ru/CeO_2-rod than that in Ru/CeO_2-cube. Combining the Raman characterization and

the structural characterizations, we found that the metal support interaction has a great influence on the Ru size formed on different supports.

In the literature reports, the formation of metal size has a great relationship with the concentration of oxygen vacancy, which presents a linear relationship with the concentration of acid site [40, 45]. Thus, we turned to characterize Ru-clusters/CeO_2, Ru/CeO_2-rod, and Ru/CeO_2-cube using NH_3-TPD to investigate the concentration of acid site of the catalyst (Fig. 6b). Obviously, the order of acid concentration of the three catalysts was in the subsequence of Ru-clusters/CeO_2 > Ru/CeO_2-rod > Ru/CeO_2-cube (Table S1). Thus, the order of the concentration of oxygen vacancy was in the subsequence of Ru-clusters/CeO_2 > Ru/CeO_2-rod > Ru/CeO_2-cube (Fig. 6c). Therefore, the smallest size of the Ru with the highest concentration of oxygen vacancy, having the largest steric hindrance, is favor to the linear adsorption mode of styrene, which is benefit to generation of linear product. Similar results are also reported before [46].

In summary, Ru-clusters/CeO_2 is used as an active catalyst for the hydromethoxycarbonylation of styrene with > 99% conversion of styrene, giving 83% and 12% regioselectivity of linear and branched ester, respectively. Structural characterizations demonstrate that the **L**/**B** ratio is related to the Ru size of supported Ru catalysts. Further Raman characterization and NH_3-TPD demonstrate that the metal support interaction and the concentration of oxygen vacancy of the catalyst have a great influence on Ru size. Mechanism investigation proves the radical path of hydromethoxycarbonylation of styrene over Ru-clusters/CeO_2. Considering the complication varying of CeO_2 shape, further research work, in-depth investigating of the factors affecting regioselectivity, is ongoing.

Acknowledgments

This work was supported by the Strategic Priority Research Program of the Chinese Academy of Sciences (XDB17020300), the National Natural Science Foundation of China (21721004, 21690084, and 21690080).

References

[1] H. Li, K. Dong, H. Jiao, H. Neumann, R. Jackstell, M. Beller, *Nat. Chem.* **2016**, *8*, 1159-1166.
[2] Y. Dou, H. Zhang, A. Zhou, F. Yang, L. Shu, Y. She, J.-R. Li, *Ind. Eng. Chem. Res.* **2018**, *57*, 8388-8395.
[3] F. E. A. Van Waes, J. Drabowicz, A. Cukalovic, C. V. Stevens, *Green Chem.* **2012**, *14*, 2776.
[4] M. Noè, A. Perosa, M. Selva, *Green Chem.* **2013**, *15*, 2252.
[5] K. Dong, X. Fang, S. Gülak, R. Franke, A. Spannenberg, H. Neumann, R. Jackstell, M. Beller, *Nat. Commun.* **2017**, *8*, 14117.
[6] L. Wu, Q. Liu, I. Fleischer, R. Jackstell, M. Beller, *Nat. Commun.* **2014**, *5*, 3091.
[7] P. Roesle, C. J. Durr, H. M. Moller, L. Cavallo, L. Caporaso, S. Mecking, *J. Am. Chem. Soc.* **2012**, *134*, 17696-17703.
[8] P. Roesle, L. Caporaso, M. Schnitte, V. Goldbach, L. Cavallo, S. Mecking, *J. Am. Chem. Soc.* **2014**, *136*, 16871-16881.
[9] K. Y. Qiang Liu, Percia-Beatrice Arockiam, Robert Franke,Henri Doucet,, a. M. B. Ralf Jackstell, *Angew. Chem. Int. Ed.* **2014**, *54*, 4493 –4497.
[10] D. B. Williams, M. L. Shaw, M. J. Green, C. W. Holzapfel, *Angew. Chem. Int. Ed.* **2008**, *47*, 560-563.
[11] X. Fang, H. Li, R. Jackstell, M. Beller, *Angew. Chem. Int. Ed.* **2014**, *53*, 9030-9034.
[12] L. Wu, Q. Liu, R. Jackstell, M. Beller, *Angew. Chem. Int. Ed.* **2014**, *53*, 6310-6320.
[13] D. B. Nielsen, B. A. Wahlqvist, D. U. Nielsen, K. Daasbjerg, T. Skrydstrup, *ACS Catal.* **2017**, *7*, 6089-6093.

[14] X. F. Wu, X. Fang, L. Wu, R. Jackstell, H. Neumann, M. Beller, *Acc. Chem. Res.* **2014**, *47*, 1041-1053.
[15] X.-F. W. Jin-Bao Peng, *Angew. Chem. Int. Ed.* **2018**, *57*, 1152-1160.
[16] M. C. Ester Guiu, Bianca MunInorga, *Organometallics*, *25*, 3102.
[17] M. Amezquita-Valencia, G. Achonduh, H. Alper, *J. Org. Chem.* **2015**, *80*, 6419-6424.
[18] W. Wang, L. Cui, P. Sun, L. Shi, C. Yue, F. Li, *Chem. Rev.* **2018**, *118*, 9843-9929.
[19] Z. He, Z. Hou, Y. Luo, Y. Dilixiati, W. Eli, *Catal. Sci. Technol.* **2014**, *4*, 1092.
[20]
[21] J. An, Y. Wang, J. Lu, J. Zhang, Z. Zhang, S. Xu, X. Liu, T. Zhang, M. Gocyla, M. Heggen, R. E. Dunin-Borkowski, P. Fornasiero, F. Wang, *J. Am. Chem. Soc.* **2018**, *140*, 4172-4181.
[22] J. An, Y. Wang, Z. Zhang, Z. Zhao, J. Zhang, F. Wang, *Angew. Chem. Int. Ed.* **2018**, *57*, 12308-12312.
[23] Y. Wang, J. Zhang, H. Chen, Z. Zhang, C. Zhang, M. Li, F. Wang, *Green Chem.* **2017**, *19*, 88-92.
[24] C. Hansch, A. Leo, R. W. Taft, *Chem. Rev.* **1991**, *91*, 165-195.
[25] M. Wang, F. Wang, J. Ma, M. Li, Z. Zhang, Y. Wang, X. Zhang, J. Xu, *Chem. Commun.* **2014**, *50*, 292-294.
[26] A. Marjasvaara, M. Torvinen, P. Vainiotalo, *J. Mass Spectrom.* **2004**, *39*, 1139-1146.
[27] A. Abad, A. Corma, H. Garcia, *Chem. Eur. J.* **2008**, *14*, 212-222.
[28] Z. Zhang, Y. Wang, M. Wang, J. Lü, L. Li, Z. Zhang, M. Li, J. Jiang, F. Wang, *Chin. J. Catal.* **2015**, *36*, 1623-1630.
[29] F. Wang, C. Li, X. Zhang, M. Wei, D. G. Evans, X. Duan, *J. Catal.* **2015**, *329*, 177-186.
[30] H. Huang, Q. Dai, X. Wang, *Appl. Catal. B Environ.* **2014**, *158-159*, 96-105.
[31] X. Zhang, R. You, D. Li, T. Cao, W. Huang, *ACS Appl. Mater. Interfaces* **2017**, *9*, 35897-35907.
[32] A. Aitbekova, L. Wu, C. J. Wrasman, A. Boubnov, A. S. Hoffman, E. D. Goodman, S. R. Bare, M. Cargnello, *J. Am. Chem. Soc.* **2018**, *140*, 13736-13745.
[33] S. Li, Y. Xu, Y. Chen, W. Li, L. Lin, M. Li, Y. Deng, X. Wang, B. Ge, C. Yang, S. Yao, J. Xie, Y. Li, X. Liu, D. Ma, *Angew. Chem. Int. Ed.* **2017**, *56*, 10761-10765.
[34] J. Chen, H. Wang, Z. Wang, S. Mao, J. Yu, Y. Wang, Y. Wang, *ACS Catal.* **2019**, *9*, 5302-5307.
[35] J. Dong, Q. Fu, Z. Jiang, B. Mei, X. Bao, *J. Am. Chem. Soc.* **2018**, *140*, 13808-13816.
[36] W. Lin, A. A. Herzing, C. J. Kiely, I. E. Wachs, *J. Phys. Chem. C* **2008**, *112*, 5942-5951.
[37] Y. Guo, S. Mei, K. Yuan, D.-J. Wang, H.-C. Liu, C.-H. Yan, Y.-W. Zhang, *ACS Catal.* **2018**, *8*, 6203-6215.
[38] X. P. Fu, L. W. Guo, W. W. Wang, C. Ma, C. J. Jia, K. Wu, R. Si, L. D. Sun, C. H. Yan, *J. Am. Chem. Soc.* **2019**, *141*, 4613-4623.
[39] Q. Dai, S. Bai, J. Wang, M. Li, X. Wang, G. Lu, *Appl. Catal. B Environ.* **2013**, *142-143*, 222-233.
[40] Z. Zhang, Y. Wang, J. Lu, J. Zhang, M. Li, X. Liu, F. Wang, *ACS Catal.* **2018**, *8*, 2635-2644.
[41] S. Zhang, C. R. Chang, Z. Q. Huang, J. Li, Z. Wu, Y. Ma, Z. Zhang, Y. Wang, Y. Qu, *J. Am. Chem. Soc.* **2016**, *138*, 2629-2637.
[42] Y. Z. Yongle Guo, Zhongkui Zhao, *Chin. J. Catal.*, **2018**, *39*, 181-189.
[43] Z. Q. W. Chang Huang, Xue Qing Gong *Chin. J. Catal.*, **2018**, *39*, 1520-1526.
[44] A. Satsuma, M. Yanagihara, J. Ohyama, K. Shimizu, *Catal. Today* **2013**, *201*, 62-67.
[45] Z. Zhang, Y. Wang, M. Wang, J. Lu, C. Zhang, L. Li, J. Jiang, F. Wang, *Catal. Sci. Technol.* **2016**.
[46] M. Nishiumi, H. Miura, K. Wada, S. Hosokawa, M. Inoue, *ACS Catal.* **2012**, *2*, 1753-1759.

Ru/CeO_2催化剂催化苯乙烯的氢甲氧基羰基化反应高选择性制备直链酯类化合物

安静华[a,b]，王业红[a]，张志鑫[a]，张健[a], Martin Gocyla[c], Rafal E. Dunin-Borkowski[c]，王峰[a,*].

[a]中国科学院大连化学物理研究所，洁净能源国家实验室，生物能源研究部，辽宁大连116023

[b]中国科学院大学，北京100049

[c]厄恩斯特·鲁斯卡电子显微与光谱学中心和彼得·格伦伯格研究所，尤利希52425，德国

摘要: 酯类化合物在工业上具有广泛的应用，例如可用于合成香水、调味剂（味精）、洗涤剂和表面活性剂等。其中，烯烃的氢烷氧基羰基化反应为一种合成酯类化合物的重要方法，由于其低消耗、100%的原子经济性和原料的易获得等优势，使其在制备酯类化合物中成为一个有效且实际可行的方法。对于该反应，文献多采用Pd或Rh的络合均相催化剂，其中，控制反应过程中直链酯类化合物和支链酯类化合物的选择性是一项颇具挑战性的课题。虽然目前可通过配体的设计和修饰来调节，但多集中在均相催化体系，因此在选择性调变方面的研究仍很欠缺。相对于均相催化，多相催化由于产物的易分离、提纯，催化剂可循环使用等优势，而逐渐引起了研究者们的广泛关注。虽然，在多相催化体系中，Pd负载在强酸性树脂作为催化剂已被报道应用于苯乙烯的氢甲氧基羰基化反应，但在该反应中支链酯类化合物为主要产物。因此，寻找一个可有效改善多相反应体系中选择性问题的方法是非常有意义的。

在本研究工作中，我们以CeO_2纳米颗粒(NP)、CeO_2纳米棒(Rod)、CeO_2纳米立方体分别为载体，利用浸渍法制备出Ru/CeO_2、Ru/CeO_2-rod、Ru/CeO_2-cube三种催化剂，并进一步用于苯乙烯的氢甲氧基羰基化反应中。我们探究了CO压力、反应温度、反应时间对三种催化剂催化苯乙烯的氢甲氧基羰基化反应的影响。研究结果表明，Ru/CeO_2为多相催化剂来催化苯乙烯的氢甲氧基羰基化反应时，苯乙烯的选择性达> 99%，直链酯的选择性为83%，支链酯的选择性为12%。机理研究表明，该反应为自由基机理。动力学分析表明，该反应的反应活化能为48.50 KJ·mol^{-1}。结合三种催化剂的不同反应活性以及HRTEM的结构表征结果得出结论，该反应中**L**/**B**比值与Ru的尺寸有较大关系。进一步的拉曼表征以及NH_3-TPD表征结果证明，Ru的尺寸与金属-载体之间的相互作用以及催化剂表面的氧空位浓度有直接关系。

关键词: 选择性；钌/二氧化铈；酯类化合物；氢甲氧基羰基化反应；烯烃；多相催化；

收稿日期: XXXX-XX-XX. 接受日期: XXXX-XX-XX. 出版日期: XXXX-XX-XX.

*通讯联系人. 电话: (0411)84379798; 传真: (0411)84379798; 电子信箱: wangfeng@dicp.ac.cn

基金来源: 中国科学院战略重点研究项目(XDB17020300); 国家自然科学基金(21721004, 21690084, 21690080)

本文的英文电子版由 Elsevier 出版社在 ScienceDirect 上出版 (http://www.sciencedirect.com/science/journal/18722067).

Graphical Abstract

Linear-Regioselective Hydromethoxycarbonylation of Styrene Using Ru-Clusters/CeO_2

Catalyst

Jinghua An[a,b], Yehong Wang[a], Zhixin Zhang[a], Jian Zhang[a], Martin Gocyla[c], Rafal E. Dunin-Borkowski[c], and Feng Wang[a,*]

[a] Dalian Institute of Chemical Physics, Chinese Academy of Sciences;

[b] University of Chinese Academy of Sciences

c Ernst Ruska Centre for Microscopy and Spectroscopy with Electrons and Peter Grünberg Institute, Forschungszentrum Juelich GmbH, Juelich 52425, Germany

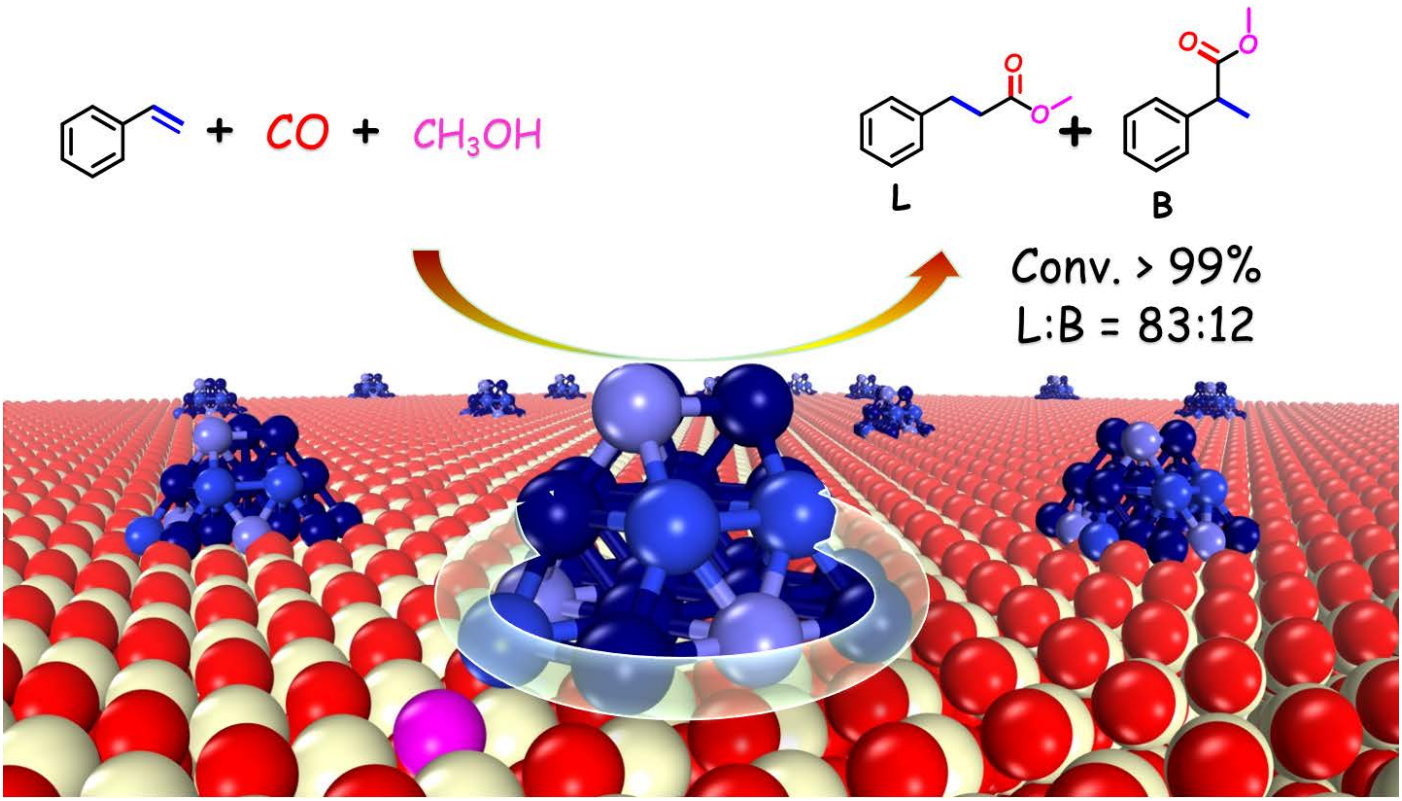

Ru-clusters/CeO_2 is prepared and first employed as a heterogeneous catalyst for the hydromethoxycarbonylation of styrene with > 99% conversion of styrene, giving 83% and 12% regioselectivity of linear and branched ester, respectively. Further systematic studies demonstrate that the **L**/**B** ratio is related to the Ru size of supported Ru catalysts. And the highest regioselectivity for linear ester can be obtained using Ru-clusters/CeO_2 as catalyst owing to the presence of the smallest Ru size on the CeO_2 surface.